ISSN 1330-3651 (Print), ISSN 1848-6339 (Online)
https://doi.org/10.17559/TV-20180721153103
Original scientific paper

A MPPT Method based on Improved Fibonacci Search Photovoltaic Array

Jun-Hong ZHANG, Xue-Ye WEI, Liang HU, Jian-Guang MA

Abstract: The P-U curve of photovoltaic arrays (PVAs) has multi-peak characteristics under uneven illumination environments, and the maximum power point tracking (MPPT) strategy for the single peak may fail. An improved Fibonacci search algorithm is proposed to carry out MPPT of photovoltaic arrays under uniform illumination or light mutation. A multiple-interval search algorithm based on a circuit analysis method is presented for different topology arrays and illumination distributions. The series array analysis adopts the current analysis method, the parallel array analysis adopts the voltage analysis method, and the series and parallel array analysis adopts the current and voltage analysis method; then, the output control volume is determined, and the search interval is divided. The search steps in the Fibonacci method and the real-time changes of parameters in the optimization process can be observed by MATLAB simulation. Experimental results show that the algorithm uses less computation time and small area search instead of global search.

Keywords: circuit analysis method; Fibonacci search; MATLAB simulation; maximum power point tracking; photovoltaic array

1 INTRODUCTION

Solar power as a renewable energy source is an important way to solve the energy crisis. It is essential to operate the PVA source at maximum power point (MPP) due to its low energy conversion efficiency. PV cells have complex nonlinear output characteristics for the influence of light intensity and temperature, but there is always only one MPP on the output curve. Many MPPT algorithms have been proposed by scholars in order to maximize the conversion of light energy into electrical energy and make the PV cells operate at the MPP. Under a uniform illumination environment (UIE), there is only one peak value on the power-voltage (P-U) curve of photovoltaic arrays. Commonly used MPPT control algorithms in this case include the constant voltage method, perturbation and observation (P&O) method and incremental conductance method [1-4]. PVAs are usually affected by shadows such as trees, billboards and black clouds in applications. The MPPT control method based on sampling data easily falls into local peaks because PV arrays output a multi-peak curve with several peaks in multi-intervals under non-uniform illumination environments (NIEs). Now, a large number of research results for multi-peak MPPT algorithms have been published. These results are mainly divided into algebraic algorithms [5-10] and artificial intelligence algorithms [11-16]. The artificial intelligence algorithms have good adaptability and accuracy independent of the specific mathematical model of the PV array. However, they require a large amount of operation data and experience accumulation developed by complex circuits. Moreover, there are random power oscillations in the MPPT process, which brings great disturbance to the load or power grid. The algebraic algorithm has a small calculation, clear MPPT search trajectory and simple circuit, but the accuracy is closely related to the mathematical model of the PV array. The error of MPPT under NIE still exists.

To overcome the limitations of the above algorithms, an improved Fibonacci search algorithm is adopted in this paper. First, the algorithm ascertains array topology, determines the type of light by measuring the data, and pre-treats the characteristic curve of the system. The range of the global MPP is narrowed directly, and the MPPT can be realized quickly under UIE. A search interval is redefined to avoid misjudgment when an abrupt illumination is detected. Dividing the multiple search intervals according to the level of illumination and the array structure under NIE, the local peaks are obtained by the improved Fibonacci algorithm in each interval. The maximum power of the whole output is obtained by comparing several local extreme values.

2 THE MATHEMATICAL MODEL OF PV ARRAY

A PV module comprises several PV batteries in series, and a PV array comprises PV modules connected in series, parallel or series parallel.

2.1 A Double-Diode Mathematical Model for PV Battery

A PV battery model based on double-diode [17] is shown in Fig. 1.

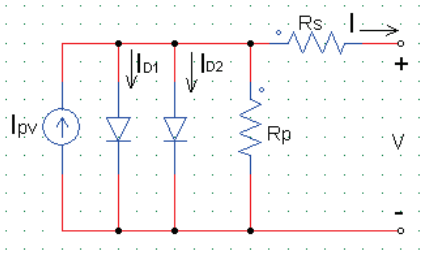

Figure 1 The equivalent circuit of double-diode model for the PV battery

$$I = I_{\mathrm{PV}} - I_{\mathrm{D1}} - I_{\mathrm{D2}} - \frac{V + R_{\mathrm{s}} I}{R_{\mathrm{p}}} \tag{1}$$

where: I_{PV} - photo current; R_{s}, R_{p} - battery equivalent series and parallel resistance.

Reverse saturable currents of diode D1 and D2 are as follows

$$I_{\mathrm{D1}} = I_{01}\left[\exp\left(\frac{V + R_{\mathrm{s}} I}{V_{\mathrm{T1}}}\right) - 1\right]$$

$$I_{D2} = I_{02}\left[\exp\left(\frac{V+R_s I}{V_{T2}}\right)-1\right]$$
$$V_{T1} = \frac{A_1 KT}{q},\ V_{T2} = \frac{A_2 KT}{q}$$

where: A_1=1, A_2=2 - ideal factors for polar tube D1 and D2; q = 1.6022×10^{-19} C - unit charge; K = 1.3806×10^{-22} J/K - Pohl-Weitzman constant; T - absolute temperature.

The expression of output I and V is as follows:

$$I = I_{PV} - I_{01}\left[\exp\left(\frac{V+R_s I}{V_{T1}}\right)-1\right]- -I_{02}\left[\exp\left(\frac{V+R_s I}{V_{T2}}\right)-1\right]-\frac{V+R_s I}{R_p} \quad (2)$$

2.2 Mathematical Model of PV Module

$$I = I_{PV} - I_{01}\left[\exp\left(\frac{V+R_{Ms} I}{N_s V_{T1}}\right)-1\right]- -I_{02}\left[\exp\left(\frac{V+R_{Ms} I}{N_s V_{T2}}\right)-1\right]-\frac{V+R_{Ms} I}{R_{Mp}} \quad (3)$$

The number of series battery N_s

$$R_M = R_{Ms}N_s,\ R_{Mp} = R_p N_s,$$
$$I_{PV} = \frac{(I_{PVn}+K_i\Delta T)G}{G_n},\ I_{PVn} = \frac{(R_{Ms}+R_{Mp})I_{scn}}{R_{Mp}}$$
$$I_{01} = I_{02} = \frac{I_{scn}+K_i\Delta T}{\exp\left[\frac{(V_{ocn}+K_V\Delta T)}{V_T}\right]-1}$$

where: open circuit voltage V_{ocn} and short circuit current I_{scn} under standard conditions; T_s (25 °C) - standard temperature, $\Delta T = T - T_s$; Illumination G and standard illumination D_s (1000 W/m^2).

2.3 The Mathematical Model of Array

The mathematical model in series array (SA) composed of N_{sa} PV modules is as follows:

$$I = I_{PV} - I_{01}\left[\exp\left(\frac{V+R_{Ms} I N_{sa}}{N_s V_{T1} N_{sa}}\right)-1\right]- -I_{02}\left[\exp\left(\frac{V+R_{Ms} I N_{sa}}{N_s V_{T2} N_{sa}}\right)-1\right]-\frac{V+R_{Ms} I N_{sa}}{N_{sa} R_{Mp}} \quad (4)$$

The mathematical model in parallel array (PA) composed of N_{pa} PV modules:

$$I = I_{PV} - I_{01}\left[\exp\left(\frac{V+R_{Ms} I/N_{pa}}{N_s V_{T1}/N_{pa}}\right)-1\right]- -I_{02}\left[\exp\left(\frac{V+R_{Ms} I/N_{pa}}{N_s V_{T2}/N_{pa}}\right)-1\right]-\frac{V+R_{Ms} I/N_{pa}}{R_{Mp}/N_{pa}} \quad (5)$$

The mathematical model in series parallel of N_{sa} and N_{pa} PV modules:

$$I = I_{PV} - I_{01}\left[\exp\left(\frac{V+R_{Ms} I(N_{sa}/N_{pa})}{N_s V_{T1}}\right)-1\right]- -I_{02}\left[\exp\left(\frac{V+R_{Ms} I(N_{sa}/N_{pa})}{N_s V_{T2}}\right)-1\right]-\frac{V+R_{Ms} I(N_{sa}/N_{pa})}{R_{Mp}(N_{sa}/N_{pa})} \quad (6)$$

3 FIBONACCI SEARCH ALGORITHM

3.1 Search Principle

If the integer sequence $\{F_n\}$ (n=0,1, ...) meets the following conditions, $\{F_n\}$ is called a Fibonacci sequence.

$$\begin{cases} F_0 = F_1 = 1 \\ F_n = F_{n-2} + F_{n-1} \end{cases}$$

F_n is the nth Fibonacci number and F_{n-1}/F_n is Fibonacci fraction. When an interval is shortened with the nth exploration point, the length shortenings are F_{n-1}/F_n, F_{n-2}/F_{n-1}, F_{n-3}/F_{n-2},…, and F_1/F_2 respectively. If the function $f(t)$ is monotonous on the interval I = [a, b] and there exists a unique number $P \in I$ such that $f(t)$ is increasing on [a, P] and decreasing on [P, b].

The Fibonacci search step is as follows:

(1) Select the initial data and determine the search interval [a, b], then calculate the search number n according to the search precision value, $\delta > 0$.

$$\frac{b-a}{F_n} \le \delta \quad (7)$$

(2) Select the initial exploration points t_1 and t_2 to satisfy $t_1 < t_2$ on the interval [a, b]:

$$\begin{cases} \frac{t_1-a}{b-a} = \frac{F_{n-2}}{F_n} \\ \frac{t_2-a}{b-a} = \frac{F_{n-1}}{F_n} \end{cases}, \text{ then}$$
$$\begin{cases} t_1 = a + \frac{F_{n-2}}{F_n}(b-a) = b + \frac{F_{n-1}}{F_n}(a-b) \\ t_2 = a + \frac{F_{n-1}}{F_n}(b-a) = b + \frac{F_{n-2}}{F_n}(a-b) \end{cases} \quad (8)$$

(3) Calculate the functions $f(t_1)$ and $f(t_2)$, as shown in Figs. 2(a) and (b).

If $f(t_1) > f(t_2)$, eliminate the interval (t_2, b) then move the search interval to the left, setting $a_1 = a$ and $b_1 = t_2$ on

the interval (a, t_2), the new test points are $t_{12} = t_1$ and $t_{11} = a_1 + \frac{F_{n-2}}{F_n}(b_1 - a_1)$.

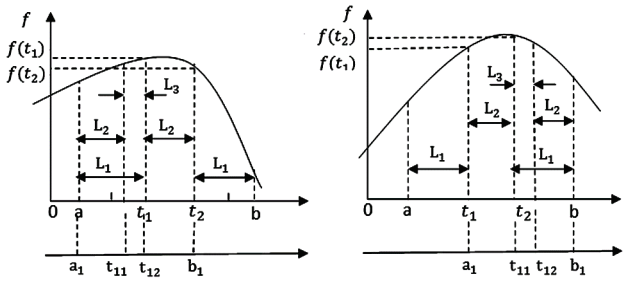

(a) Move to the left (b) Move to the left

Figure 2 Fibonacci search diagram

If $f(t_1) < f(t_2)$, eliminate the interval (a, t_1) then move the search interval to the left, setting $a_1 = t_1$ and $b_1 = b$ on the interval (a, t_2), the new test points are $t_{11} = t_2$ and $t_{12} = a_1 + \frac{F_{n-1}}{F_n}(b_1 - a_1)$.

The values of the Fibonacci sequence are $F_n = L_1$, $F_{n-1} = L_2$, and $F_{n-2} = L_3$.

(4) Set $f(t)$=max ($f(t_1)$, $f(t_2)$), the function $f(t)$ is the maximum value of the search interval as $n-2=0$.

The algorithm is an accurate one-dimensional search method of variable step size with a high computational efficiency which uses symmetry to construct the step length. The target function is calculated only once in the search process so that the computational efficiency is high. There is no need to search the entire output voltage range of the PV array, which improves the response speed of the MPPT and reduces the power loss for disturbance. Based on a precise mathematical model, the algorithm can ensure the accuracy of the search results and is suitable for the hardware structure of the traditional MPPT.

3.2 The Improved Fibonacci Search Method

The improved Fibonacci method is described as follows:

(1) Increase the end conditions and reduce the search numbers

The value of the function $f(t)$ is very sensitive to the independent variable t, and small changes of t will make $f(t)$ have a larger error in the vicinity of the MPP. In general, the smaller the tolerance Delta δ is, the more accurate the results are and the longer search times are. Taking $|t_1 - t_2| \le \delta$ and $|f(t_1) - f(t_2)| \le \delta$ as the terminating conditions can significantly reduce the search times under the same δ.

(2) The final value is determined by the bisection search method

In order to further improve the accuracy of the results, the single bisection search method is used to determine the final $f(t)$ according to the $N-1$ search results, which can reduce the error caused by the concussion near the MPP.

(3) Sectioning search on multi-intervals

The multi-intervals are divided according to the topology and illumination distribution of photovoltaic arrays and each interval has only one local extreme point. Then, the improved Fibonacci method is used in each subinterval to MPPT, and the global MPP is obtained. It can eliminate the faulty judgment theoretically and can be applied to any topological photovoltaic array under non-uniform illumination.

(4) When the illumination changes, the parameters are initialized again to determine the new search interval according to the measured illumination variation value.

4 IMPLEMENTATION OF THE MPPT ALGORITHM

The entire interval of the PV array under a UIE and the subinterval under the NIE meet the single peak characteristics of output. The variable t can express the output voltage or current according to the topology of the array, and the $f(t)$ is the output power of the array. The control flow chart of the MPPT with improved Fibonacci is shown in Figs. 3 and 4. First, determine the topology of the array and judge the illumination environment of the array, then judge whether the illumination mutation occurs according to the change of illumination and output power, which decide whether to redefine the search interval to cope with the uncertainty of the external environment.

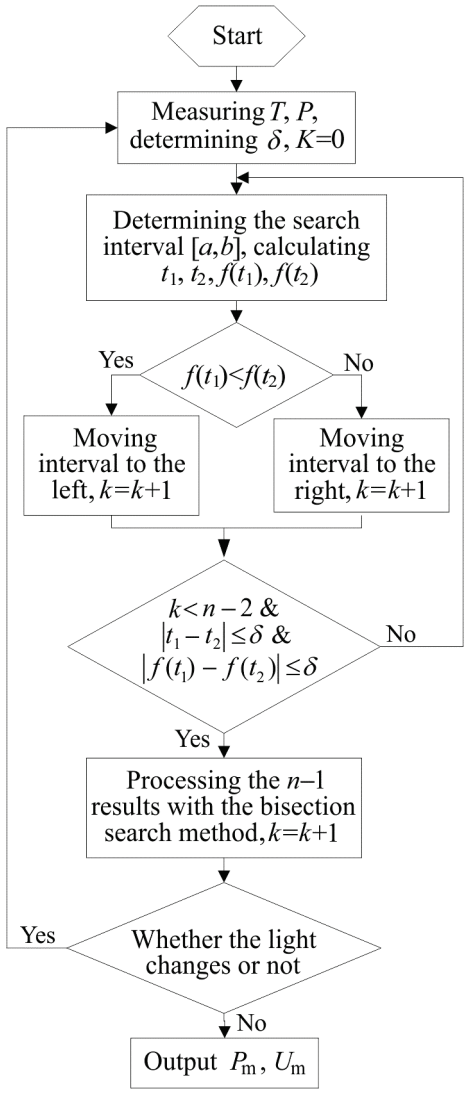

Figure 3 MPPT flow chart of the Fibonacci search under UIE

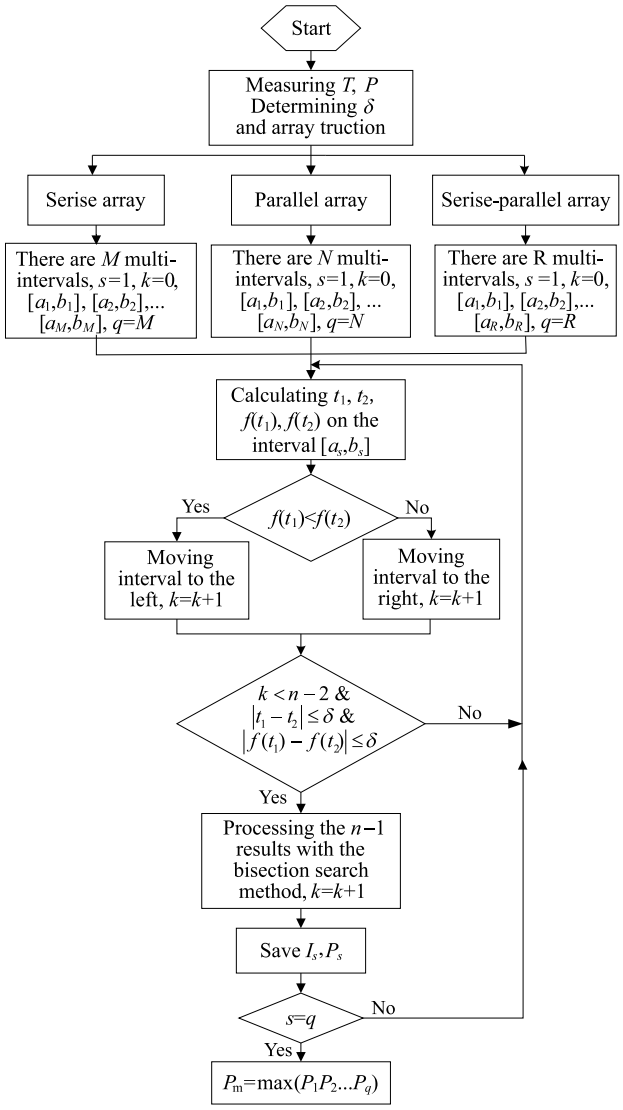

Figure 4 MPPT flow chart of the Fibonacci search under NIE

4.1 UIE

The relationship between the MPP voltage V_m of PVAs and the open circuit voltage V_{ocn} meets $V_m \approx 0.8 \cdot V_{ocn}$ under UIE. As an example of the KG200GT PV module, the electrical parameters for an improved double-diode model are shown in Tab. 1.

Table 1 Electrical parameters for improved double-diode model

Parameter name	Value
Battery structure	$N_s = 54$
Maximum power P_m	270 W
Voltage of maximum power V_m	26.3 V
Current of maximum power I_m	7.63A
Reverse saturable current I_0	4.128×10^{-10} A
Photocurrent I_{PV}	8.22 A
Series resistance R_s	0.335 Ω
Parallel resistance R_p	155.48 Ω

The simulation uses a single module in order to compare with the module standard output P_m and V_m. Parameters from Tab. 1 are brought into the formula (3) and the simulation experiment is carried out by the m file of MATLAB according to the flow chart of Fig. 3. The output voltage is controlled and the initial voltage interval parameters are set as follows: $G = 1000$ W/m^2, $T = 25$ °C, $a = 0.75 \cdot V_{ocn} = 24.675$ V, $b = 0.85 \cdot V_{ocn} = 27.965$ V, $\delta = 0.01$. The search process is shown in Tab. 2. The local output curve of the tracking results is shown in Fig. 5.

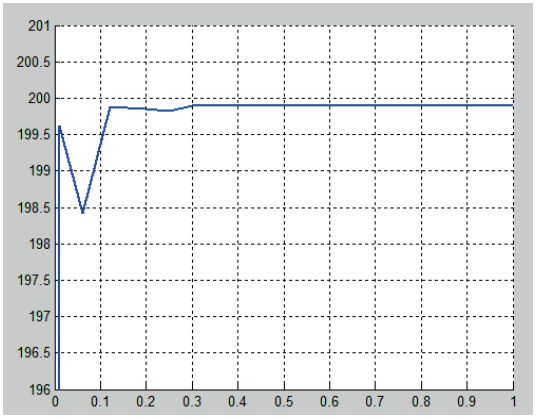

Figure 5 A local magnification chart of *P-t* for *P*=1000 W/m^2

When searching for $k = 5$, $t_1 = 26.2289$ V, $t_2 = 199.8918$ V, $f(t_1) = 199.8862$ W, $f(t_2) = 199.8918$ W, the final result t is found by the single bisection method. That is, $t = (t_2 + t_1)/2 = 26.2604$ V, $f(t) = 199.9018$ W. The difference ΔP_m between $f(t)$ and the standard value P_m is 0.0982 W. The error ΔV_m between t and V_m is 0.0504 V. The tracking time t is 0.3 s.

When the illumination changes, such as from $G = 1000$ W/m^2 to 600 W/m^2, the power also changes. For example, when setting the $\Delta P = 0.2$, when the power change value is greater than the ΔP, the illumination should be remeasured, and the search interval is defined. The search process is described in Tab. 2, and the power output curve is shown in Fig. 6. The new interval parameters are: $\delta = 0.01$, $a = 0.75 \cdot V_{oc2} = 24.15$ V, $b = 0.85 \cdot V_{oc2} = 27.37$ V. V_{oc2} is the open circuit voltage of the illumination of 600 W/m^2 and V_{oc2} is 32.19 V.

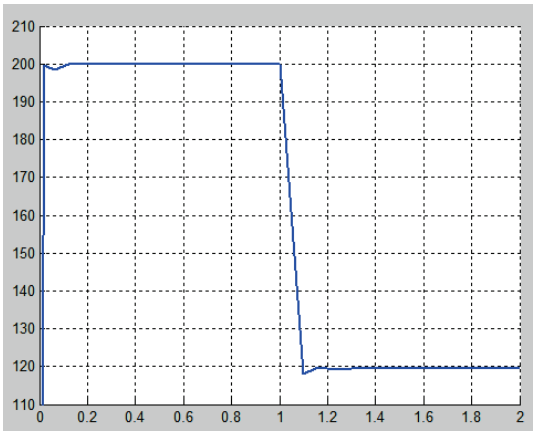

Figure 6 Local magnification of *P-t* curve when illumination changes

The search results are: $t = (t_2 + t_1)/2 = 26.5639$ V, $f(t) = 119.6276$ W. Ideally, the maximum power of the module P_m is 119.6699 W and V_m is 26.5554 V under 600 W/m^2, ΔP_m is 0.0423 W. The tracking time is adjusted to 0.4 s. Thus, it can be seen that the Fibonacci search can track quickly and accurately to the MPP as the illumination changes. From Tab. 1, it is not advisable to expand the search range in the traditional method, when the direction of the two searches is the same. Because even light does not change, the search interval is not alternating directions

each step instead it is moving two or three times in one direction, which causes miscarriage of Justice. In practical applications, the change values of detection illumination and power are used to define the interval, so that the search speed is faster and the result is more accurate.

4.2 NIE

According to the flow chart in Fig. 4, the MPPT of the arrays with different topological structures is discussed respectively under NIE.

4.2.1 SA

Taking two modules in series as an example, the parameters are as follows: G_1 = 1000 W/m^2, G_2 = 600 W/m^2, I_{cs1} = 8.2279A, I_{cs2} = 4.9367 A. The current analysis method is adopted as the current of the series module is equal. The output voltages are the sum of the output voltage of two modules, which can be calculated by the formula (4). In SA, the illumination level determines the number of local extreme points, which can be predicted by [0.8·I_{cs}, I_{cs}], and the location of the global MPP is related to the illumination distribution and module number [18]. Therefore, the MPPT is realized by controlling the output current. The power curve has two local power extremes under two illumination levels. When the output current is on the interval [0, I_{cs1}], the two modules supply the power simultaneously, and there is a local power point P1. When the current is on the interval [I_{cs1}, I_{cs2}], due to the bypass diode, only G_2 supplies the power, and there is another local point P2. Therefore, there are two search intervals, such as those in Tabs. 3 and 4, the search curve is shown in Fig. 7. In the detection point distribution shown in Fig. 8, the red and blue dots represent points t_1 and t_2 respectively. The MPP is calculated by two local extremes. In the first interval, a=0.8·I_{cs1}=6.5823A, b = I_{cs1} = 8.2279 A, δ = 0.01. The local MPP P1 is: t = 7.7788 A, $f(t)$ = 204.2908 W. Ideally, P1 is 204.301 W and ΔP1 is 0.01 W.

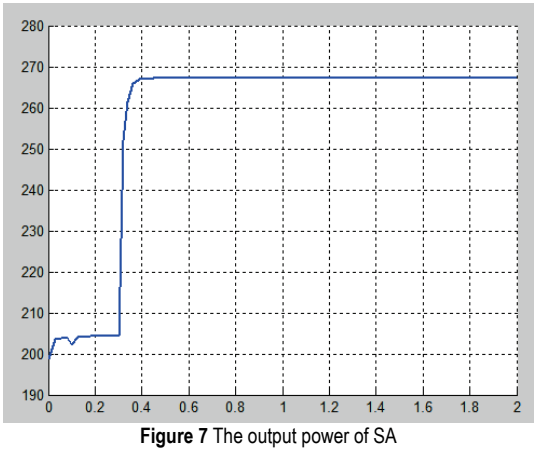

Figure 7 The output power of SA

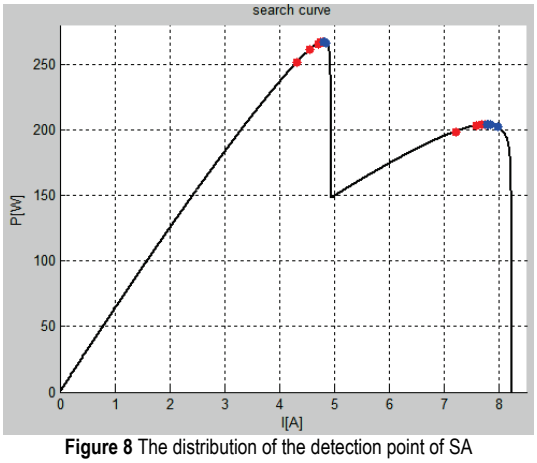

Figure 8 The distribution of the detection point of SA

Table 2 Search data records under UIE

Search times K	Detection points		Function values		Moving direction	Conditions	
	t_1	t_2	$f(t_1)$	$f(t_2)$		$t_2 - t_1$	$\lvert f(t_1) - f(t_2)\rvert$
0	25.9329	26.7071	199.6131	199.4025		0.7742	0.2106
1	25.4520	25.9329	198.4228	199.6131	left	0.4809	1.1903
2	25.9329	26.2289	199.6131	199.8862	right	0.296	0.2731
3	26.2289	26.4093	199.8862	199.8488	right	0.1804	0.0014
4	26.1116	26.2289	199.8251	199.8862	left	0.1173	0.0611
5	26.2289	26.2902	199.8862	199.8918	right	0.0613	0.0056

Table 3 The search data record of the current in the interval [0, I_{cs1}]

Search times K	Detection points		Function values		Moving direction	Conditions	
	t_1	t_2	$f(t_1)$	$f(t_2)$		$t_2 - t_1$	$\lvert f(t_1) - f(t_2)\rvert$
	7.2115	7.5987	198.9348	203.5744		0.3872	4.6396
1	7.5987	7.8393	203.5744	204.1471	right	0.2406	0.5727
2	7.8393	7.9882	204.1471	202.2712	right	0.1489	1.8759
3	7.7485	7.8393	204.2756	204.1471	left	0.0906	0.1285
4	7.6889	7.7485	204.1080	204.2756	left	0.0596	0.1676
5	7.7485	7.7791	204.2756	204.2907	right	0.0306	0.0151
6	7.7791	7.8090	204.2907	204.2506	right	0.0299	0.0401
7	7.7788	7.7791	204.2908	204.2907	left	0.0003	0.0001

In the second interval, a = 0.8·I_{cs2} = 3.9494 A, b = I_{cs2} = 4.9367 A, δ = 0.01. The local MPP P2 is: t = 4.8110 A, $f(t)$ = 267.3118 W. Ideally, P2 is 267.3211 W and ΔP1 is 0.0093 W, P_m = max(P1, P2) = 267.3118 W.

As shown in Fig. 8, in the two illumination conditions, the SA output presents two peaks, and the global MPP is 267.3118 W. As seen in Fig. 7, the first local MPP is achieved at 0.3 s and the second at 0.5 s, which completes the entire search process in 0.6 s with a fast search speed

and stable output power. Similarly, M ranges of [$0.8 \cdot I_{cs1}$, I_{cs1}], [$0.8 \cdot I_{cs2}$, I_{cs2}], …, [$0.8 \cdot I_{csM}$, I_{csM}] are divided when illumination level values are arranged from big to small under the M illumination levels in SA. Then, the global MPP can be derived from M local extremum points. It is obviously difficult for the traditional Fibonacci algorithm to find the global MPP even if the search interval is enlarged in the case of multi-level illumination and multiple local extremums points. The improved Fibonacci search can overcome the limitations of traditional algorithms and can be used for MPPT with any level of illumination.

Table 4 The search data record of the current in the interval [I_{cs1}, I_{cs2}]

Search times	Detection points		Function values		Moving direction	Conditions	
K	t_1	t_2	$f(t_1)$	$f(t_2)$		$t_2 - t_1$	$\|f(t_1) - f(t_2)\|$
0	4.3269	4.5592	252.0919	261.4954		0.2323	9.4035
1	4.5592	4.7036	261.4954	265.9131	right	0.1714	4.4177
2	4.7036	4.7929	265.9131	267.2937	right	0.0893	1.3806
3	4.7929	4.8471	267.2937	266.8541	right	0.0542	0.4396
4	4.7574	4.7929	266.9504	267.2937	left	0.0355	0.3897
5	4.7929	4.8112	267.2937	267.3112	right	0.0183	0.0175
6	4.8112	4.8290	267.3112	267.1830	right	0.0178	0.1282
7	4.8110	4.8112	267.3118	267.3112	left	0.0002	0.0006

Table 5 The search data record of PA

Search times	Detection points		Function values		Moving direction	Conditions	
K	t_1	t_2	$f(t_1)$	$f(t_2)$	Left/Right	$t_2 - t_1$	$\|f(t_1) - f(t_2)\|$
0	26.1508	27.1071	328.0953	326.0107		0.9563	2.0846
1	25.8520	26.1508	327.1590	328.0953	left	0.2988	0.9363
2	26.1508	26.3329	328.0953	328.2603	right	0.1821	0.165
3	26.3329	26.6289	328.2603	328.1314	right	0.2960	0.1289
4	26.2703	26.3329	328.2537	328.2603	left	0.0626	0.0066
5	26.3329	26.3899	328.2603	328.2503	right	0.0570	0.0100
6	26.3301	26.3329	328.2672	328.2603	left	0.0028	0.0009

4.2.2 PA

Taking two modules in parallel as an example, the parameters are as follows: G_1 = 1000 W/m^2, G_2 = 600 W/m^2, V_{oc1} = 32.9 V, V_{oc2} = 32.2 V. The output voltage of the parallel modules is equal, and the voltage analysis method is adopted. The output current is the sum of the two modules calculated by Eq. (5). Therefore, the MPPT is realized by controlling the output voltage. If the output voltage of each module for the parallel array is equal, the output power is superimposed on the output power of each module. If not equal, the output voltage and power will be superimposed by the maximum output voltage and power of the parallel modules. The output curve has a single peak characteristic, which is close to the UIE, and the level of illumination determines the composition number of the line segment [17]. Because the open circuit voltage is mainly related to the temperature, it is less affected by the illumination and the equation of $V_{oc} = V_{oc1}$ is adopted. The initial parameters for the search interval are: $a = 0.75 \cdot V_{oc1}$ = 24.6750 V, $b = 0.85 \cdot V_{oc1}$ = 29.6100 V, δ = 0.01. The search process and the curve are shown in Tab. 5 and Fig. 9.

The MPP is: t = 26.3315 V, $f(t)$ = 328.2675 W/m^2. The ΔP is 0.0092 W compared with the theoretical value P = 328.2767 W. The output voltage of PA under two illumination levels has a turning point due to the series blocking diode, which causes the curve to be composed of two parts. The output curve is composed of M sections for a parallel array with an arbitrary illumination level of M, but the single peak characteristic does not change, which makes MPPT implementation easier, the tracking accuracy higher and the speed faster.

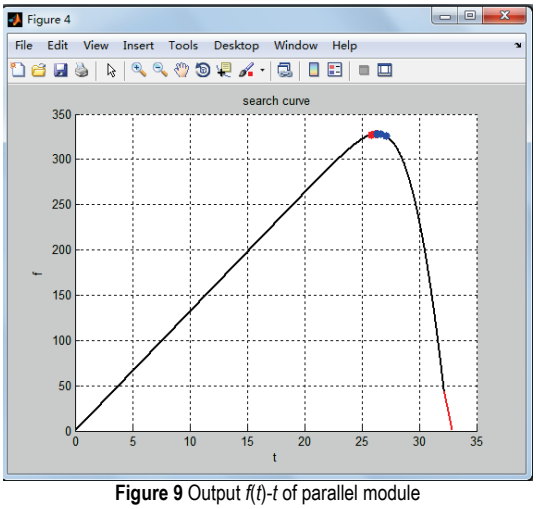

Figure 9 Output $f(t)$-t of parallel module

4.2.3 SPA

Taking 2×2 photovoltaic arrays as an example, the parameters are as follows: G_1 = 1000 W/m^2, G_2 = 600 W/m^2 in branch I, $G_1 = G_2$ = 1000 W/m^2 in branch II. The current analysis method used in series branch and voltage analysis method used in parallel branch, the current interval is divided into two parts, [0, I_{cs2}] and [I_{cs2}, I_{cs1}]. The two models output power of branch I in the interval [0, I_{cs2}], the output voltage is $V = V_{11} + V_{12}$, the current is I_1. The voltage is equal in parallel branches, and the current I_2 of branch II can be calculated from the voltage of branch I. The output power of the array is calculated using formula (6), that is $P = V(I_1 + I_2)$. Only the G_1 module works in branch I, and two modules works in branch II, so the output voltage in branch I is greater than branch II in the interval

[I_{cs2}, I_{cs1}]. Only branch II outputs power since the blocking diode is reversed cut-off. The corresponding voltage V is calculated from the current value I of the detection points by taking the current as the search interval. The improved Fibonacci algorithm is used to carry out local MPPT for SPA on the interval [0, I_{cs2}] and [I_{cs2}, I_{cs1}], then the MPP can be obtained. The voltage value is calculated in a large current range to ensure that the search voltage interval is completely covered and the extreme points can be determined rapidly. The initial interval for search is: a = 2.0000 A, b = 4.9460 A in the current interval [0, I_{cs2}]. The voltages are calculated by the current detection points.The search process is shown in Tab. 6.

Table 6 The SPA search data record in the interval [0, I_{cs2}]

Search times K	current interval		Current detection points		voltage detection points		Moving direction	Conditions	
	a	b	t_1	t_2	V_1	V_2	Left/Right	$t_2 - t_1$	$\|f(V_1) - f(V_2)\|$
0	2.0000	4.9460	3.1264	3.8196	60.9476	59.6108		0.6932	85.9829
1	3.1264	4.9460	3.8196	4.2503	59.6108	58.5040	left	0.4307	53.6256
2	3.8196	4.9460	4.2503	4.5169	58.5040	57.5470	left	0.2666	33.8666
3	4.2503	4.9460	4.5169	4.6784	57.5470	56.7032	left	0.1615	21.0700
4	4.5169	4.9460	4.6784	4.7851	56.7032	55.8505	left	0.1607	14.0955
5	4.6784	4.9460	4.7851	4.8390	55.8505	55.1835	left	0.0539	6.8322
6	4.7851	4.9460	4.8390	4.8924	55.1835	54.0297	left	0.0534	5.0294
7	4.8390	4.9460	4.8924	4.8925	54.0297	54.0258	left	0.0001	0.0050

Table 7 SPA searching data record in the interval [I_{cs2}, I_{cs1}]

Search times$K$	current interval		Current detection points		voltage detection points		Moving direction	Conditions	
	a	b	t_1	t_2	V_1	V_2	Left/Right	$t_2 - t_1$	$\|f(V_1) - f(V_2)\|$
0	4.9460	8.2289	6.2012	6.9737	29.6702	28.7509		0.7725	8.9444
1	6.2012	8.2289	6.9737	7.4536	28.7509	27.9239	right	0.4799	0.8305
2	6.9737	8.2289	7.4536	7.7490	27.9239	27.1603	right	0.2954	3.9535
3	6.9737	7.7490	7.2701	7.4536	28.2794	27.9239	left	0.1835	0.3843
4	6.9737	7.4536	7.1572	7.2701	28.4711	28.2794	left	0.1129	0.2432
5	7.1572	7.4536	7.2701	7.3403	28.2794	28.1508	right	0.0702	0.0182
6	7.1572	7.3403	7.2272	7.2701	28.3543	28.2794	left	0.0429	0.0557
7	7.2272	7.3403	7.2701	7.2970	28.2794	28.2310	right	0.0269	0.0098
8	7.2701	7.3403	7.2970	7.3134	28.2310	28.2009	right	0.0164	0.0041
9	7.2701	7.3134	7.2867	7.2970	28.2497	28.2310	left	0.0103	0.0014
10	7.2867	7.3134	7.2970	7.2974	28.2310	28.2197	right	0.0004	0.0006

Local MPP P1 is: t = 4.8925 A, $f(V)$ = 669.8263 W, which is compared with the theoretical value P_1 = 69.8743 W, the ΔP is 0.048 W.

When the current is in [I_{cs2}, I_{cs1}], the initial search interval is: a = I_{cs2} = 4.9460 A, b = I_{cs1} =8.2289 A. The search process is shown in Tab. 7 and the output P-V curve is shown in Figs. 10 and 11.

Local MPP P2 is: t = 7.2972 A, $f(V)$ = 438.2817 W, which is compared with the theoretical value 438.2911 W and the ΔP is 0.094 W.

As shown in Figs. 10 and 11, the output of the SPA shows the current characteristics in the current range, and there are 2 local extreme points under two illumination levels, which are located in two current ranges. Red and blue dots represent detection points t_1 and t_2 respectively. The output curve shows parallel characteristics in the voltage range which is composed of three curves in three voltage intervals [17]. In M×N SPA, first the current intervals are determined according to the level of illumination, the voltage interval is determined according to the parallel branch. Then, the values of the voltage detection points are calculated by the current detection points, and finally the power is calculated. To track the whole search interval, the whole current interval is taken to ensure that the local extreme points have corresponding convergent voltage values.

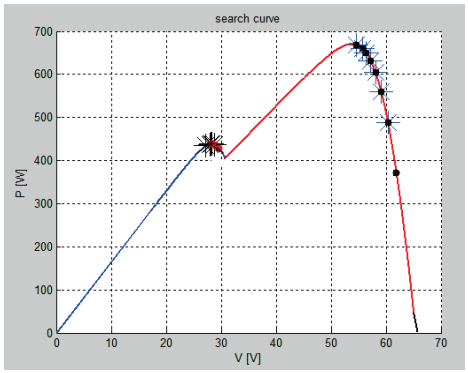

Figure 10 P-V output curve of SPA

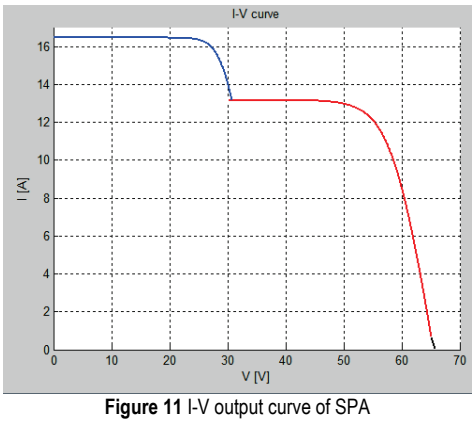

Figure 11 I-V output curve of SPA

5 CONCLUSION

The MPPT algorithm based on an improved Fibonacci search is proposed based on the accurate mathematical model of PV arrays and increased measurement of environmental parameters. The parameters are used to judge the change and distribution of light in order to provide a basis for MPPT. The MPP is tracked quickly and accurately by dividing the multiple tracking intervals and determining the control voltage or current, and the system is stable at the MPP under the condition of NIV. The algorithm has good anti-interference ability. It can track the global MPP for any environment and PV array topology and improve the output efficiency of PV arrays.

Acknowledgements

This paper is supported by the Fundamental Research Funds for Beijing University of Civil Engineering and Architecture (X18011) and D funded project to cultivate talents in Beijing City (No. 2013D005017000008).

6 REFERENCES

[1] Zhang, X. & Cao, R. (2010). *Solar photovoltaic grid-connected power generation and its inverter control*. Beijing: Mechanical Industry Press.

[2] Zhang, J. H. & Wei, X. Y. (2013). Research on improved MPPT control algorithm for photovoltaic cell array. *Journal of Beijing Jiaotong University, 158*(37), 12-16.

[3] Nie, X. H. & Jun, L. J. (2018). Overview of global maximum power point tracking control method for photovoltaic array under partial shadow. *Power System Technology, 38*(12), 3279-3285.

[4] Spertino, F., Ahmad, J., Ciocia, A., Di Leo, P., Murtaza, A. F., & Chiaberge, M. (2015). Capacitor charging method for I–V curve tracer and MPPT in photovoltaic systems. *Solar Energy, 119*, 461-473. https://doi.org/10.1016/j.solener.2015.06.032

[5] Kouchaki, A., Iman-Eini, H., & Asaei, B. (2013). A new maximum power point tracking strategy for PV arrays under uniform and non-uniform insolation conditions. *Solar Energy, 91*, 221-232. https://doi.org/10.1016/j.solener.2013.01.009

[6] Zhou, L., Chen, Y., Guo, K., & Jia, F. (2011). New approach for MPPT control of photovoltaic system with mutative-scale dual-carrier chaotic search. *IEEE Transactions on Power Electronics, 26*(4), 1038-1048. https://doi.org/10.1109/TPEL.2010.2078519

[7] Zadeh, M. J. Z. & Fathi, S. H. (2017). A new approach for photovoltaic arrays modeling and maximum power point estimation in real operating conditions. *IEEE Transactions on Industrial Electronics, 64*(12), 9334-9343. https://doi.org/10.1109/TIE.2017.2711571

[8] Heydari-Doostabad, H., Keypour, R., Khalghani, M. R., & Khooban, M. H. (2013). A new approach in MPPT for photovoltaic array based on extremum seeking control under uniform and non-uniform irradiances. *Solar Energy, 94*, 28-36. https://doi.org/10.1016/j.solener.2013.04.025

[9] Messalti, S., Harrag, A. G., & Loukriz, A. E. (2015). *A new neural networks MPPT controller for PV systems.*In The Sixth International Renewable Energy Congress (pp. 1-6). Sousse, Tunisia.

[10] Latham, A. M., Pilawa-Podgurski, R., Odame, K. M., & Sullivan, C. R. (2013). Analysis and optimization of maximum power point tracking algorithms in the presence of noise. *IEEE Transactions on Power Electronics, 28*(7), 3479-3494. https://doi.org/10.1109/TPEL.2012.2211038

[11] Ramaprabha, R., Balaji, M., & Mathur, B. L. (2012). Maximum power point tracking of partially shaded solar PV system using modified Fibonacci search method with fuzzy controller. *International Journal of Electrical Power & Energy Systems, 43*(1), 754-765. https://doi.org/10.1016/j.ijepes.2012.06.031

[12] Koutroulis, E. & Blaabjerg, F. (2012). A new technique for tracking the global maximum power point of PV arrays operating under partial-shading conditions. *IEEE Journal of Photovoltaics, 2*(2), 184-190. https://doi.org/10.1109/JPHOTOV.2012.2183578

[13] Mohanty, S., Subudhi, B., & Ray, P. K. (2016). A new MPPT design using grey wolf optimization technique for photovoltaic system under partial shading conditions. *IEEE Transactions on Sustainable Energy, 7*(1), 181-188. https://doi.org/10.1109/TSTE.2015.2482120

[14] Ramaprabha, R. & Mathur, B. (2011). Soft computing optimization techniques for solar photovoltaic arrays. *ARPN: Journal of Engineering and Applied Sciences, 6*(10), 70-75.

[15] Chowdhury, S. R., & Saha, H. (2010). Maximum power point tracking of partially shaded solar photovoltaic arrays. *Solar Energy Materials and Solar Cells, 94*(9), 1441-1447. https://doi.org/10.1016/j.solmat.2010.04.011

[16] Alajmi, B. N., Ahmed, K. H., Finney, S. J., & Williams, B. W. (2013). A maximum power point tracking technique for partially shaded photovoltaic systems in microgrids. *IEEE Transactions on Industrial Electronics, 60*(4), 1596-1606. https://doi.org/10.1109/TIE.2011.2168796

[17] Zhang, J. H., Wei, X. Y., & Hui, Z. N. (2014). Study on the characteristics of photovoltaic large array based on the double diode model. *Advanced Materials Research, 834*, 1145-1149

[18] Zhang, J. H., Wei, X. Y, & Zhu, T. L (2015). Research on the output characteristics of photovoltaic array under the non-uniform light. *International Journal of Control and Automation, 8*(10), 431-444. https://doi.org/10.14257/ijca.2015.8.10.39

Contact information:

Jun-Hong ZHANG, lecturer, doctoral student
Deputy Director of the Research Office of Intelligent Control Theory and System
1) School of Electronic and Information Engineering, Beijing Jiaotong University,
2) School of Electrical and Information Engineering,
Beijing University of Civil Engineering and Architecture,
Beijing, 100044, China
E-mail: zhangjunhong@bucea.edu.cn

Xue-Ye WEI, professor
Beijing Jiaotong University,
School of Electronic and Information Engineering,
Beijing, 100044, China
E-mail: xywei@bjtu.edu.cn

Liang HU, doctoral student
Beijing Jiaotong University,
School of Electronic and Information Engineering,
Beijing, 100044, China
E-mail: 13111047@bjtu.edu.cn

Jian-guang MA, doctoral student
Beijing Jiaotong University
School of Electronic and Information Engineering,
Beijing, 100044, China
E-mail: 14111042@bjtu.edu.cn